IRSTI: 53.49.19



Y. Kambarov*

Research Center «Surface Engineering and Tribology», S. Amanzholov EKU, 070002, Republic of Kazakhstan, Ust-Kamenogorsk, 34 30th Guards Division Street *e-mail: yedilzhan@mail.ru

EFFECT OF SPRAYING REGIME AND VACUUM ANNEALING ON THE MICROSTRUCTURE AND WEAR RESISTANCE OF PLASMA-SPRAYED COCRFENIMN HIGH ENTROPY COATINGS

Abstract: In this study, coatings based on a high-entropy CoCrFeNiMn alloy were deposited on 316L stainless steel substrates using air plasma spraying with two different regimes. After spraying, the coatings were vacuum annealed at 500° C. The aim of the work was to study the effect of hydrogen flow rate and subsequent annealing on the phase composition, microstructure, and mechanical properties of the coatings. X-ray phase analysis showed that a face-centered cubic (FCC) structure dominates in all samples, but after annealing, especially in the regime APS 2, the formation of σ -phase and oxide phases MnO and MnCr₂O₄ is observed. According to SEM/EDS data, a layered microstructure typical for air plasma sprayed coatings and an increased oxygen content in the upper zone of the coatings after annealing were established. The highest microhardness of 390 HV_{0·2} was recorded for the APS 2a coating, which is associated with the formation of hard secondary phases. However, wear tests showed that the best wear resistance was observed in coatings obtained using the APS 1 and APS 1a regimes, due to a more stable phase structure and a lower tendency to oxidation. The results obtained emphasize the importance of comprehensive optimization of spraying parameters and annealing conditions to improve the performance characteristics of HEA based coatings under friction and wear conditions.

Key words: high entropy alloys, coating, air plasma spraying, mechanical properties, microstructure.

Introduction

High-entropy alloys (HEAs), which typically include five or more major elements in equimolar or near-equimolar ratios with high mixing entropy, are the subject of growing research interest each year. HEAs have attracted considerable attention due to their exceptional properties, such as outstanding mechanical characteristics [1, 2], ultra-high strength [3], high ductility [4], high corrosion resistance, and excellent wear resistance [5, 6]. The development and study of HEA with high wear resistance is of interest both for fundamental science and for critically important practical applications. Among the various HEAs developed, the CoCrFeNiMn alloy, also known as the Cantor alloy, is of particular interest. It forms a single-phase solid solution with a face-centered cubic (FCC) crystal lattice [7]. However, according to data [2], CoCrFeMnNi and Al_{0.3}CoCrFeNi alloys exhibit increased wear rates relative to aluminum oxide at room temperature, which is due to the relative softness of the FCC structure. The work [8] shows that the addition of 0.5 mol of Mn to the AlCrFeNiTi alloy leads to a decrease in wear resistance due to an increase in the wear coefficient.

To date, most HEAs have been obtained using traditional technologies such as melting, casting, and powder metallurgy methods [4]. However, the use of thermal spraying opens up new possibilities for the formation of HEA based coatings, allowing materials to be deposited on a wide range of substrates at high speed and with good adhesion. At the same time, issues related to the optimization of spraying parameters and ensuring stable performance characteristics of such coatings remain unresolved.

In addition to varying the chemical composition, one of the effective ways to modify the properties of HEA coatings (HEC) is annealing. In particular, vacuum annealing can significantly improve the structure and properties of coatings. The work [9] shows that optimizing the annealing parameters of high-velocity oxygen fuel (HVOF) coatings based on CoCrFeMnNi contributes to increased strength. Studies [10-12] also confirmed that vacuum annealing after deposition significantly reduces porosity, improves microstructural homogeneity, and increases the quality of interphase bonding due to the intensification of diffusion processes. Elevated temperatures promote phase redistribution and defect elimination, which ultimately leads to improved wear resistance of the coatings.

A number of studies demonstrate the successful application of thermal spraying technologies for the formation of coatings based on HEA. The work [13] investigates the evolution of phases in

the CoCrFeNiMn coating after laser remelting. Coatings containing Ni, Co, Fe, Cr, Si, Al, and Ti obtained by APS and HVOF spraying demonstrated high oxidation resistance at 1100 °C due to the formation of a protective α -Al₂O₃ phase [14]. Similar results were obtained for coatings containing Ni, Co, Fe, Cr, Si, Al, and Ti [15], where after annealing at 1100 °C for 10 hours, a significant increase in hardness and resistance to grain growth was observed [16]. The wear resistance of the CoCrFeNiMn HVOF coating was studied at different temperatures [9, 17]. Other works considered isothermal oxidation and tribological behavior of AlCoCrFeNi and FeCoNiCrMn coatings obtained by cold gas dynamic spraying [18].

Despite the accumulated experimental experience, the effect of vacuum annealing on the microstructure and tribological properties of HEA based coatings obtained by APS remains insufficiently investigated. The main mechanisms underlying the change in properties depending on the annealing conditions are also unclear. Thus, an urgent task remains to improve the performance characteristics of such coatings by optimizing technological parameters, including the consumption of plasma-forming gas and the heat treatment regime.

In this work, high-entropy CoCrFeNiMn alloy coatings were applied to 316L stainless steel substrates by air-plasma spraying and subsequently subjected to vacuum annealing at 500 °C. The mechanical properties of the coatings were investigated using microindentation and wear resistance assessment methods, which allowed the properties of the coating to be analyzed at various structural levels. The results of the experiments provided a comprehensive understanding of the microstructure, phase composition, and mechanical characteristics of the coatings, confirming their potential for use under conditions of increased loads and wear.

Materials and Methods

The starting material for the coating, in the form of a CoCrFeNiMn powder alloy, was prepared using an industrial high-pressure gas atomization method. Fig. 1 shows SEM and EDS maps of the CoCrFeNiMn powder. EDS maps for each element (Mn, Co, Cr, Fe, Ni) demonstrated uniform distribution across the powder particles with no visible segregation. Each element was present in almost equal atomic proportions, confirming the homogeneity of the powder. As can be seen, the particles have a spherical shape. This shape promotes uniform powder delivery during plasma spraying. Particles ranging in size from 32 μ m to 45 μ m were selected by particle sieving.

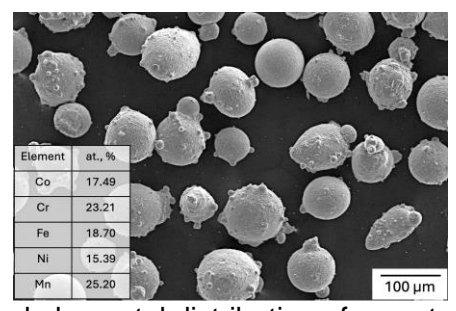


Figure 1 – Microstructure and elemental distribution of gas atomized CoCrFeNiMn powder

CoCrFeNiMn coatings were obtained by APS using an SX-60 plasma torch. Coatings were obtained at two secondary gas (hydrogen, H_2) flow rates of 1.7 and 1.9 L/min, respectively. The other spraying parameters included: arc current – 500 A, main gas (Ar) flow rate – 45 L/min, powder feed gas (N_2) flow rate – 8 L/min, and spraying distance – 100 mm. AISI 316L stainless steel was used as the substrate.

After APS spraying, the samples were cooled in air and then annealed in a vacuum furnace. The vacuum in the furnace was created to a level of 5×10^{-5} Pa using a vacuum pump. The samples were subjected to isochronous annealing at a temperature of 500° C. The duration of isochronous annealing was 2 hours, with the heating rate maintained at 10° C per minute. After annealing, the samples were cooled in a vacuum to room temperature. The coatings in their initial state, obtained at hydrogen flow rates of 1.7 L/min and 1.9 L/min, were designated APS 1 and APS 2, and the corresponding coatings after annealing were designated APS 1a and APS 2a.

X-ray diffraction (XRD) analysis of the powder and coating was performed on a PANalytical X'PertPRO diffractometer with Cu K α radiation (λ = 0.154056 nm). The scanning range was from 20° to 90°, with a scanning speed of 0.02°/s. The obtained data were analyzed using HighScore Plus software to determine the crystal lattice parameters and phase composition.

The microstructure of the powder and the cross-section of the samples were studied using a CIQTEK SEM3200 autoemission scanning electron microscope at an accelerating voltage of 15 keV and a working distance of 10 mm. The chemical composition was analyzed using Bruker XFlash 730M-300 energy dispersive X-ray spectroscopy (EDS).

The microhardness of the HECs was determined using the Vickers method with a METOLAB 502 microhardness tester at a load of 200 mN and an exposure time of 10 s. The average thickness of the coatings was about 100 μ m. To increase the accuracy of the measurements, each coating was tested six times; the measurement points were arranged in a 3 × 3 matrix, and the distance between adjacent points was 40 μ m.

The wear tests of the HEA coatings were performed using the ball-on-disc method with an Anton Paar TRB3 tribometer, where a 5 mm diameter 100Cr6 ball slid over the coating surface. The tests were conducted at a normal load of 10 N, an oscillation frequency of 30 Hz, a stroke length of 5 mm, and a total sliding length of 100 m. The temperature during the test was 23 °C, and the relative humidity was 62%. The amount of wear in the worn tracks was measured using an AMETEK Taylor Hobson Surtronic S-100 Series profilometer.

Results and discussion

X-ray phase analysis was performed to analyze the phase composition of CoCrFeNiMn coatings obtained under various air plasma spraying (APS) conditions and subsequent annealing. The obtained diffractograms are shown in Fig. 2. The initial CoCrFeNiMn powder exhibits a single-phase structure with a face-centered cubic (FCC) lattice, which is confirmed by the presence of characteristic peaks at $2\theta \approx 43.5^{\circ}$, 50.6° , and 74.3° , corresponding to reflections from the (111), (200) and (220) planes, respectively.

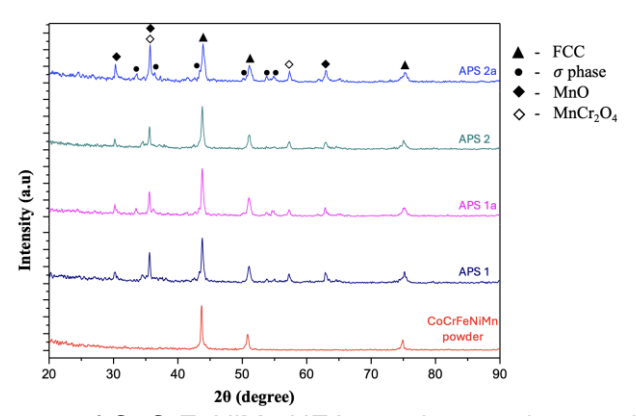


Figure 2 – XRD patterns of CoCrFeNiMn HEA powder, coatings and annealed coatings

In all sprayed coatings, the FCC phase is preserved, but an oxide peak appears at 35.6°, which intensifies after annealing, indicating an increase in the oxide content. MnCr $_2$ O $_4$ and MnO phases were also detected. However, the nature and intensity of the additional peaks vary significantly depending on the spraying regime used and subsequent annealing. APS 1 and APS 2 coatings obtained without annealing demonstrate a stable FCC structure without pronounced secondary phases. This indicates the preservation of a homogeneous solid solution in both spraying regimes. After annealing at 500 °C, additional σ -phase peaks are observed in the coating, especially in APS 2a. The σ phase is an intermetallic compound formed as a result of phase segregation, mainly along the chromium. Its presence may indicate the initial signs of solid solution decomposition. It should be noted that in the APS 2a sample – i.e., after the spraying regime APS 2 and annealing – the largest number of secondary phases was recorded, including both intermetallic and oxide components. This indicates that APS 2a leads to enhanced phase transformations, probably due to higher energy density or particle temperature. Annealing at 500 °C promotes the nucleation of the σ phase and oxides.

Figure 3 shows the microstructure of the coatings, clearly revealing the characteristic layered structure typical of coatings formed by the APS method. In APS 1 coating (Fig. 3a), a relatively homogeneous structure with clearly defined boundaries of flattened particles is observed. The porosity is moderate, and the contact between the particle layers is dense. After annealing APS 1a (Fig. 3b), the structure becomes more compact, and the number of pores decreases slightly, which may be due to the activation of diffusion processes and partial recrystallization. In the case of the

coating obtained under the APS 2 regime (Fig. 3c), a greater number of rounded pores and irregularities are observed, and the particles themselves appear less melted compared to APS 1. This may indicate differences in the temperature and velocity of the particles at the moment of impact. APS 2a (Fig. 3d) has a more porous and heterogeneous structure, with pronounced formation of oxide inclusions.

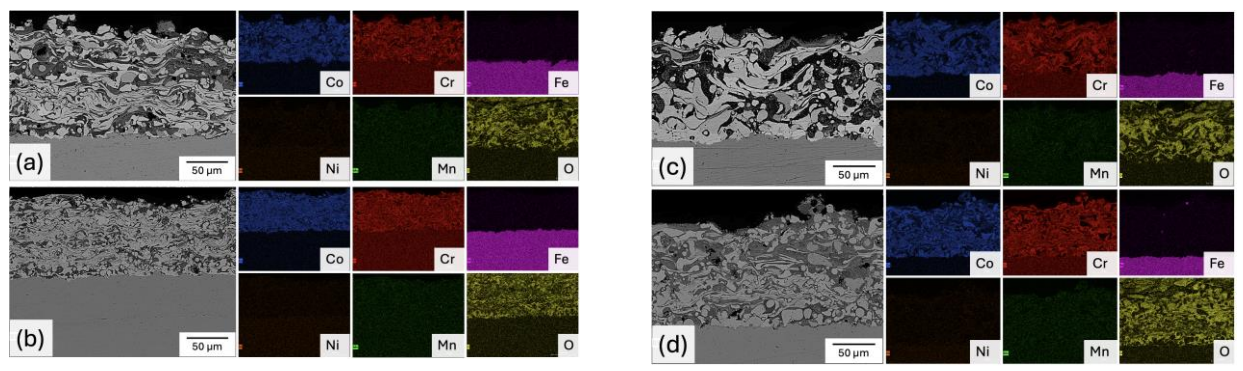


Figure 3 – Cross-sectional images with EDS maps of CoCrFeNiMn HECs: (a) APS 1, (b) APS 1a, (c) APS 2 and (d) APS 2a

The distribution of the main elements (Co, Cr, Fe, Ni, Mn, and O) across the coating cross-section is also shown in Fig. 3. In all samples, a fairly uniform distribution of Co, Cr, Fe, Ni, and Mn is observed, which confirms the preservation of the chemical homogeneity of the original HEA. However, in the samples after annealing, a significant increase in oxygen content is observed, mainly in the upper part of the coating. This indicates the formation of oxide phases, which is consistent with the results of X-ray phase analysis and may be due to either oxygen penetration during heating or oxidation of unstable components such as Mn and Cr. In addition, areas of local enrichment of Cr and Mn are visually observed in the APS 2 and APS 2a coatings, which may be associated with the onset of solid solution decomposition and the formation of secondary phases, such as the σ phase or MnCr₂O₄-type oxides.

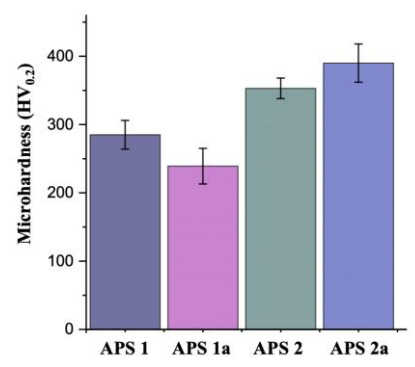


Figure 4 – Microhardness of CoCrFeNiMn HECs and annealed coatings

The microhardness of CoCrFeNiMn HEC coatings obtained under various APS regimes, as well as after annealing, is shown in Figure 4. Measurements were performed with a load of 200 g $(HV_{0.2})$ taking into account statistical error.

The coating obtained under the APS 1 deposition regime demonstrates an average microhardness of about 280 HV $_{0\cdot2}$, which corresponds to the characteristic level for high-entropy alloys with a BCC structure. However, after annealing, a decrease in microhardness to ~250 HV $_{0\cdot2}$ is observed. This may be due to recrystallization, a decrease in residual stresses and possible grain growth, as well as partial decomposition of the solid solution.

The highest microhardness values were recorded for the APS 2a coating – about 390 HV $_{0\cdot2}$, which significantly exceeds all other samples. This increase may be associated with the formation of secondary phases (σ -phase, MnO and MnCr $_2$ O $_4$ oxides) detected in X-ray phase analysis. Their presence contributes to strengthening through the mechanism of dispersion hardening. The APS 2 coating also demonstrates high hardness – about 350 HV $_{0\cdot2}$, which is probably due to the higher kinetic energy of the particles and the dense structure formed during spraying in APS 2.

Figure 5 shows the results of abrasive wear tests, expressed as the specific wear rate for coatings obtained under various APS regimes, with and without subsequent annealing. Coatings formed under APS 1 and after APS 1a annealing show the lowest wear rates – about 3.3×10⁻⁴ mm³N⁻¹m⁻¹ and 3.1×10⁻⁴ mm³N⁻¹m⁻¹ respectively. This indicates the high wear resistance of these coatings. A slight decrease in wear after annealing may be due to improved cohesion between the coating particles, reduced porosity, and increased density due to diffusion compaction.

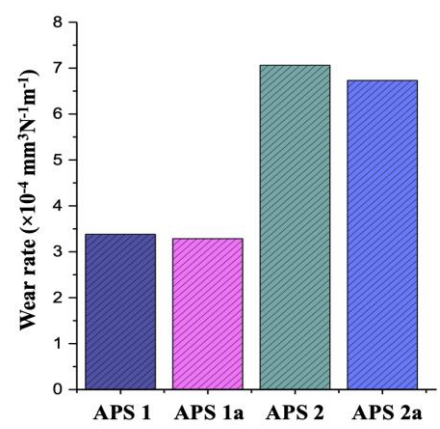


Figure 5 – Wear rates of CoCrFeNiMn HECs and annealed coatings.

In contrast, coatings obtained under the APS 2 regime and after annealing APS 2a show significantly higher wear rates $-7.0\times10^{-4}~\text{mm}^3\text{N}^{-1}\text{m}^{-1}$ and $6.8\times10^{-4}~\text{mm}^3\text{H}^{-1}\text{m}^{-1}$, respectively. Although the APS 2a sample showed the highest microhardness, its wear resistance was lower than that of all other samples. This may be due to increased brittleness, the formation of oxide phases (MnO, MnCr₂O₄), and σ -phase interphase boundaries identified in XRD analysis, which together contribute to the destruction of the coating during friction.

Conclusion

This work presents a comprehensive study of the influence of air plasma spraying regimes and subsequent annealing at 500°C on the phase composition, microstructure, and mechanical properties of coatings based on a high-entropy CoCrFeNiMn alloy. It was found that all coatings retain the main FCC phase, but in the APS 2 spraying regimes and APS 2a annealing, the formation of secondary phases – σ -phase and MnO and MnCr₂O₄ oxides – is observed.

SEM/EDS analysis showed that annealing contributes to an increase in oxygen content in the upper zone of the coating and may be accompanied by local enrichment of Cr and Mn. The highest microhardness was recorded in the APS 2a coating, which is associated with the formation of strengthening phases. However, the wear resistance of this coating was lower than that of APS 1 and APS 1a coatings, which is explained by increased brittleness and the development of phase heterogeneity.

Thus, the best balance between microhardness and wear resistance is achieved when using the APS 1 spraying and annealing regime. The results obtained emphasize the importance of optimizing spraying and annealing parameters when designing coatings based on high-entropy alloys for tribological applications.

References

- 1. Yeh J.W. Alloy design strategies and future trends in high-entropy alloys / J.W. Yeh // Jom. 2013. V. 65, V. 12. P. 1759-1771.
- 2. The sliding wear behaviour of CoCrFeMnNi and AlxCoCrFeNi high entropy alloys at elevated temperatures / J. Joseph et al // Wear. 2019. T. 428. P. 32-44.
- 3. Tensile yield strength of a single bulk Al0. 3CoCrFeNi high entropy alloy can be tuned from 160 MPa to 1800 MPa / B. Gwalani et al // Scripta Materialia. 2019. T. 162. P. 18-23.
- 4. Development and exploration of refractory high entropy alloys A review / O.N. Senkov et al // Journal of materials research. 2018. T. 33, V. 19. P. 3092-3128.
- 5. An investigation on the wear and corrosion resistance of AlCoCrFeNi high-entropy alloy coatings enhanced by Ti and Si / Z. Li et al // Surface and Coatings Technology. 2024. T. 487. P. 130949.
- 6. Corrosion resistance of CoCrFeNiMn high entropy alloy coating prepared through plasma transfer arc claddings / P.H. Gao et al // Metals. 2021. T. 11, V. 11. P. 1876.

- 7. Microstructural development in equiatomic multicomponent alloys / B. Cantor et al // Materials Science and Engineering: A. 2004. T. 375. P. 213-218.
- 8. Nong Z.S. Wear and oxidation resistances of AlCrFeNiTi-based high entropy alloys / Z.S. Nong, Y.N. Lei, J.C. Zhu // Intermetallics. 2018. T. 101. P. 144-151.
- 9. Sun H. Unveiling the effect of vacuum heat treatment on HVOF-sprayed high entropy cantor alloy coatings: Microstructure, diffusion behavior and mechanical property / H. Sun, H. Ding, T. Liu // Journal of Materials Research and Technology. 2024. T. 33. P. 9033-9043.
- 10. Function of Si on the microstructure, mechanical property and high temperature corrosion resistance of TiAlMoNbWSix HEA film / H. Zhang et al // Materials Chemistry and Physics. 2024. T. 319. P. 129336.
- 11. Investigation of hardness, tribological and adhesion properties of TiAlNiVN HEA films heat treated at different temperatures / A.M. Yılmaz et al // Tribology International. 2024. T. 197. P. 109739.
- 12. Wear-induced microstructural evolution in CoCrNi-based high-entropy alloys at cryogenic temperature / Y. Geng et al // Materials Science and Engineering: A. 2024. T. 894. P. 146185.
- 13. Phase evolution and solidification cracking sensibility in laser remelting treatment of the plasma-sprayed CrMnFeCoNi high entropy alloy coating / C. Wang et al // Materials & Design. 2019. T. 182. P. 108040.
- 14. On the study of thermal-sprayed Ni0. 2Co0. 6Fe0. 2CrSi0. 2AlTi0. 2 HEA overlay coating / W.L. Hsu et al // Surface and Coatings Technology. 2017. T. 316. P. 71-74.
- 15. Thermal sprayed high-entropy NiCo0. 6Fe0. 2Cr1. 5SiAlTi0. 2 coating with improved mechanical properties and oxidation resistance / W.L. Hsu et al // Intermetallics. 2017. T. 89. P. 105-110.
- 16. The microstructure and strengthening mechanism of thermal spray coating NixCo0. 6Fe0. 2CrySizAlTi0. 2 high-entropy alloys / L.M. Wang et al // Materials Chemistry and Physics. 2011. T. 126, V. 3. P. 880-885.
- 17. Wear behavior of HVOF-sprayed Al0. 6TiCrFeCoNi high entropy alloy coatings at different temperatures / L. Chen et al // Surface and Coatings Technology. 2019. T. 358. P. 215-222.
- 18. Deposition of FeCoNiCrMn high entropy alloy (HEA) coating via cold spraying / S. Yin et al // Journal of Materials Science & Technology. 2019. T. 35, V. 6. P. 1003-1007.

Research funding

This research was funded by the Science Committee of the Ministry of Science and Higher Education of the Republic of Kazakhstan (Grant No. AP22787411).

Е.Е. Қамбаров*

«Беттік инженерия және трибология» F3O, С. Аманжолов атындағы университет, 070002, Қазақстан Республикасы, Өскемен қаласы, 30-Гвардиялық дивизия көшесі, 34 *e-mail: yedilzhan@mail.ru

ПЛАЗМАЛЫҚ ТОЗАҢДАТУ ӘДІСІМЕН АЛЫНҒАН COCRFENIMN ЖОҒАРЫ ЭНТРОПИЯЛЫ ЖАБЫНДАРДЫҢ МИКРОҚҰРЫЛЫМЫНА ЖӘНЕ ТОЗУҒА ТӨЗІМДІЛІГІНЕ ТОЗАҢДАТУ ЖӘНЕ ВАКУУМДЫҚ КҮЙДІРУ РЕЖИМІНІҢ ӘСЕРІ

Бұл зерттеуде жоғары энтропиялы CoCrFeNiMn қорытпасы негізіндегі жабындар 316L тот баспайтын болаттан жасалған төсеніштерге екі түрлі режимде ауа-плазмалық тозаңдату арқылы жағылды. Тозаңдатудан кейін жабындар 500°С температурада вакуумдық күйдіруге ұшырады. Жұмыстың мақсаты сутегі ағынының жылдамдығы мен кейінгі күйдірудің жабынның фазалық құрамына, микроқұрылымына және механикалық қасиеттеріне әсерін зерттеу болды. Рентгендік фазалық талдау барлық үлгілерде гранецентрленген кубтық (ГЦК) құрылым басым екенін көрсетті, бірақ күйдіруден кейін, әсіресе APS 2 режимінде о-фазасы мен MnO және MnCr2O4 оксидтік фазаларының түзілуі байқалды. СЭМ/ЭРС деректері бойынша ауа-плазмалық тозаңдатумен тозаңдатылған жабынға тән қабатты микроқұрылым және қыздырудан кейін жабынның жоғарғы аймағында оттегінің жоғарылауы анықталды 390 HV0,2 ең жоғары микроқаттылық APS 2а жабындысы үшін тіркелді, бұл қатты екіншілік фазалардың пайда болуымен байланысты. Дегенмен, тозуға сынаулар көрсеткендей, ең жақсы тозуға төзімділік APS 1 және APS 1а режимдерін қолдана отырып алынған жабындарда байқалды, өйткені фазалық құрылым тұрақтырақ және тотығуға бейімділігі аз. Алынған нәтижелер үйкеліс және тозу жағдайында ЖЭҚ негізіндегі жабындардың

пайдалану сипаттамаларын жақсарту үшін тозаңдату параметрлері мен жұмсарту шарттарын кешенді оңтайландырудың маңыздылығын көрсетеді.

Түйін сөздер: жоғары энтропиялық қорытпалар, жабын, ауа-плазмалық бүрку, механикалық қасиеттер, микроқұрылым.

Е.Е. Камбаров*

НИЦ «Инженерия поверхностей и трибология», Университет имени С. Аманжолова, 070002, Республика Казахстан, г. Усть-Каменогорск, ул.30-ой Гвардейской дивизии, 34 *e-mail: yedilzhan@mail.ru

ВЛИЯНИЕ РЕЖИМА НАПЫЛЕНИЯ И ВАКУУМНОГО ОТЖИГА НА МИКРОСТРУКТУРУ И ИЗНОСОСТОЙКОСТЬ ВЫСОКОЭНТРОПИЙНЫХ ПОКРЫТИЙ COCRFENIMN ПОЛУЧЕННЫХ МЕТОДОМ ПЛАЗМЕННОГО НАПЫЛЕНИЯ

В данном исследовании покрытия на основе высокоэнтропийного сплава CoCrFeNiMn были нанесены на подложки из нержавеющей стали 316L с помощью воздушно-плазменного напыления с двумя различными режимами. После напыления покрытия были подвергнуты вакуумному отжигу при 500°C. Целью работы было изучение влияния скорости потока водорода и последующего отжига на фазовый состав, микроструктуру и механические свойства покрытий. Рентгеновский фазовый анализ показал, что во всех образцах преобладает гранецентрированная кубическая (ГЦК) структура, но после отжига, особенно в режиме APS 2, наблюдается образование σ-фазы и оксидных фаз MnO и MnCr $_2$ O $_4$. По данным P $_2$ M/ $_2$ PC установлена слоистая микроструктура, типичная для напыленных воздушно-плазменным распылением покрытий, и повышенное содержание кислорода в верхней зоне покрытий после отжига. Наибольшая микротвердость 390 $HV_{0,2}$ была зафиксирована для покрытия APS 2a, что связано с образованием твердых вторичных фаз. Однако испытания на износ показали, что наилучшая износостойкость наблюдалась у покрытий, полученных с использованием режимов APS 1 и APS 1a, благодаря более стабильной фазовой структуре и меньшей склонности к окислению. Полученные результаты подчеркивают важность комплексной оптимизации параметров напыления и условий отжига для улучшения эксплуатационных характеристик покрытий на основе ВЭС в условиях трения и износа.

Ключевые слова: высокоэнтропийные сплавы, покрытие, воздушно-плазменное напыление, механические свойства, микроструктура.

Information about the authors

Yedilzhan Yerzhanuly Kambarov – Researcher at RC «Surface engineering and Tribology», S. Amanzholov East Kazakhstan University, Ust-Kamenogorsk, Republic of Kazakhstan; e-mail: yedilzhan@mail.ru. ORCID: https://orcid.org/0000-0002-0838-6724.

Авторлар туралы мәліметтер

Еділжан Ержанұлы Қамбаров – «Беттік инженерия және трибология» ҒЗО ғылыми қызметкері, С. Аманжолов атындағы Шығыс Қазақстан университеті, Өскемен, Қазақстан Республикасы; e-mail: yedilzhan@mail.ru. ORCID: https://orcid.org/0000-0002-0838-6724.

Сведения об авторах

Едилжан Ержанулы Камбаров — Научный сотрудник НИЦ «Инженерия поверхности и трибология», Восточно-Казахстанский Университет имени С. Аманжолова, Усть-Каменогорск, Республика Казахстан; e-mail: yedilzhan@mail.ru. ORCID: https://orcid.org/0000-0002-0838-6724.

Received 04.08.2025 Revised 14.08.2025 Accepted 18.08.2025